1988

Cyclic tests of full-scale composite joint subassemblages, 1988

Seung-Joon Lee

Le-Wu Lu

CYCLIC TESTS OF FULL-SCALE COMPOSITE JOINT SUBASSEMBLAGES

by Seung-Joon Lee[1] and Le-Wu Lu[2], Member, ASCE

ABSTRACT: Three full-scale composite joint subassemblages, representing parts of the six-story prototype test structure, were built and tested cyclically under a program of controlled displacements. The specimens included two flange joints, one exterior and one interior, and one exterior web joint. The tests were conducted to study the stiffness, strength, ductility and energy dissipation capacity of the subassemblages with emphasis on the effects of the composite slab and the panel zone deformation. Theoretical predictions of the subassemblage behavior have been developed and compared with the test results.

INTRODUCTION

The overall plan of the Steel Structure Phase of the U.S. - Japan Cooperative Research Program Utilizing Large-Size Testing Facilities (Foutch, et al. 1987, Roeder, et al. 1987) included the testing of structural members, joints, subassemblages as well as reduced-scale building models. Three full-size beam-to-column joint subassemblages, which were replicas of parts of the six-story prototype structure, were tested under cyclic loading in the Fritz Engineering Laboratory of Lehigh University.

---

[1]Asst. Prof. of Architecture, Ajou Univ. Suweon, Korea, formerly Res. Assoc., Dept. of Civ. Engrg., Lehigh University, Bethlehem, PA 18015
[2]Prof. of Civ. Engrg., Lehigh University, Bethlehem, PA 18015

The beams in two of the specimens were connected to the column flanges and the web panels of the joints were unreinforced for shear. In the third specimen, the column was oriented for weak-axis bending and a full moment-resisting web connection was provided. All the specimens had a steel deck supported concrete slab acting compositely with the beam.

A major goal of the tests was to develop information which could be used in study of the lateral drift characteristics of multistory steel structures. The drift characteristics represent the fundamental knowledge required in a seismic response analysis and are influenced by stiffness properties of the structural elements. Figure 1 shows the components of the total drift of a beam-to-column joint subassemblage. The total drift Δ_t can be separated into three components: column component, beam component and panel zone component

$$\Delta_t = \Delta_c + \Delta_b + \Delta_p \tag{1}$$

in which Δ_c is the drift caused by the bending and shear deformation of the columns, Δ_b the drift caused by the deformation of the beams and Δ_p the drift caused by panel zone deformation. In order to properly evaluate the stiffness and drift characteristics of a building structure, it is necessary to develop a full understanding of the behavior of the structural components and to establish analytical models to represent the behavior. The three specimens included in this study were so selected that the relative importance of the three drift components may be systematically examined.

DESCRIPTION OF TEST SPECIMENS

Three joint subassemblages were selected from the third floor (level Z_4) of the prototype structure, where the preliminary design studies

indicated that significant inelastic deformations would occur (Askar et al. 1983). They are designated as (1) EJ-FC, exterior joint, flange connection, (2) IJ-FC, interior joint, flange connection, and (3) EJ-WC, exterior joint, web connection. EJ-FC and IJ-FC were from Frame B and EJ-WC from Frame A (or C). EJ-FC joined girder G_2 to column C_4, and IJ-FC girders G_2 to column C_5, and EJ-WC girder G_1 to column C_1, which was oriented for weak-axis bending. The details of the specimens are shown in Figs. 2, 3 and 4.

The design of the joints of the prototype was carried out primarily in Japan, where the applicable Architectural Institute of Japan (AIJ) Standards (Standards for design of steel structures, 1970) allowed inelastic shear distortion in the panel zone of joints. Shear stiffening was therefore not provided in the joints. In fact, calculations showed that, in a large number of the joints, panel zone distortion would develop before yielding of the adjoining members. In the selection of the test specimens, considerable attention was given to the relative magnitude of panel zone deformation and its effect on overall joint behavior. The behavior of IJ-FC was expected to be dominated by panel zone distortion, with the columns remaining essentially elastic. In EJ-WC, joint shear distortion would be relatively small because the applied shear was resisted by two column flanges instead of a single column web. EJ-FC represented an intermediate case in that the shear distortion would be important but not overly dominant. Inelastic deformations would occur in the beam and columns as well as the panel zone.

The height of the columns of the test specimens was 3.4 m., which was the story height of the prototype structure. This selection was made by assuming that the points of contraflexure occurred at the mid-heights of the adjacent stories. The length of beams was 2.3 m., measured from the point of load application to the center line of the column. This length was chosen

after considering the available space on the laboratory test floor and the capacity of the jacks used in testing. The beam flanges were welded either directly to the column flange (EJ-FC and IJ-FC) or to the connecting plates (EJ-WC). It should be noted that the cope holes, which allowed continuous welding of the beam flanges, appeared to be somewhat larger than those specified in the U.S. fabrication practice. The web of the beam was bolted to a shear plate with five 5/8 in. diameter A325 bolts tightened by the turn-of-nut method. A constant slab width of 1.2 m., was selected for all the specimens. The effective slab widths of the girders in the exterior and interior frames of the prototype were 0.777 m. and 1.873 m., respectively, according to the American Institute of Steel Construction (AISC) Specification (Specification for design, fabrication and erection of structural steel for buildings, 1978). Two stub beams were attached to the column at the joint in the transverse direction to simulate the transverse girders in the prototype. They were extended to the edges of the slab and connected to the column web by bolting (shear connection). To develop the composite action between the beam and the slab, two 130 mm long and 22.0 mm (7/8 in.) diameter headed shear studs were welded through the metal deck to the beam flange in each rib. All the other properties of the prototype joints were closely duplicated in the test specimens.

TEST SETUP AND PROCEDURE

The basic setup included of a test frame and a loading system (Fig. 5). The test frame, consisting of beams, columns and diagonal braces, was designed to be sufficiently stiff to minimize the lateral movement of the upper hinge support. The lower hinge support was fastened directly to the test floor.

A vertical displacement-controlled load was applied by a mechanical jack at each end of the beam. The jack was mounted on the pedestal and was connected to the beam through a load cell. The maximum stroke of the jack was 300 mm in each direction and the capacity was 200 kN. Figure 6(a) shows the cyclic displacement program adopted for testing. The peak point in each direction is denoted as LP n^+ or LP n^- (LP = Load Point). The procedure of selecting the displacement program was first suggested by Plumier (Plumier, 1983). Figure 6(b) explains the basic concept: The "yield load" P_y^+ or P_y^- is determined as the intersection of two tangents of the predicted monotonic load-deformation curve. One is the tangent at the origin, K_o, and the other is the tangent having a slope $K_o/10$. The corresponding Δ_y^+ and Δ_y^- are obtained from the predicted curves as shown. The smaller of the two, designated as Δ_y, was used as reference in the loading program. At the beginning, increments of $\Delta_y/5$ were used with 3 cycles at each increment. After the first 15 cycles, the displacement was then incremented in steps of Δ_y. This procedure was repeated until failure occurred. For IJ-FC, the same displacement was applied at the ends of both beams.

The instrumentation of the specimens was designed to determine the applied loads, to check the reactions at the supports, and to measure the deformation and internal stresses of the specimens. Figure 7 shows the instrumentation of EJ-FC. The applied displacements were controlled by a dial gage, and the corresponding loads were measured by the load cell. Dial gages were installed at the four corners of the panel zone to measure vertical and horizontal displacements of those points. These readings were used to study the shear deformation of the panel zone. Strain gages were placed on the beams and columns. Readings from the strain gages mounted on the column flanges were used to determine shear forces in the columns, which

were the horizontal reactions at the hinge supports. The beam was gaged at section's between shear connectors. Two electrical clip gages and four electrical rotational gages were attached to measure the relative slip between the concrete slab and steel beam and the rotation of the beam, respectively. Also, a mechanical rotational gage was welded to the end of the beam to measure the rotation at that point.

A B&F data acquisition system was used to collect the data from the electrical instruments. The data were then recorded on paper tapes of a teletype machine and transferred to the mini-computer, MINC, for processing and plotting.

SPECIMEN BEHAVIOR AND TEST RESULTS

The test results of the three specimens are presented as the load-deformation relationships in Figs. 8, 9, and 10. The numbers at the peaks indicate the cycle numbers as shown in Fig. 6(a). The hysteresis diagrams, characterizing the overall behavior of specimen and the behavior of its components, are as follows:

P- Δ_t: Hysteresis diagram of the overall behavior of specimen

P- θ_b: Hysteresis diagram of composite beam rotation

P- γ_p: Hysteresis diagram of panel zone distortion

P- Δ_c: Hysteresis diagram of column component

where P is the applied load, Δ_t the total deflection of the specimen (measured at the load point), θ_b the rotation of the composite beam, γ_p the average shear distortion of the panel zone, and Δ_c the column component of the total deflection.

The diagrams can be transformed to other types of plots such as the end moment versus rotation (M_b - θ_b) diagrams for the composite beams, and the

panel zone moment versus distortion diagrams. The columns in EJ-FC and IJ-FC experienced very limited inelastic deformation and their behavior is therefore not described here.

Joint EJ-FC: A total of 28 displacement cycles were applied and the specimen remained essentially elastic through the first 9 cycles (the first 15 cycles were the nominal elastic cycles). At cycle 10^+ (upward loading), the lower beam flange started to yield at a measured stress of 0.71 σ_y, where σ_y is the yield stress of the flange material. This was followed by web panel yielding at the middle height occurring during cycle 10^- (downward loading). The measured shear stress was $0.8\tau_y$, where τ_y is the yield stress in shear of the web material, given by the von Mises yield criterion. Residual stresses were believed to be the cause of early yielding which, however, did not result in significant changes of stiffness. Web yielding spread rather rapidly during the next cycle, and the panel became completely plastified at cycle 16^+. The lower beam flange was extensively yielded and yielding also occurred in the column flange at the level of the beam flange. Slip of the beam web connection bolts and concrete cracking along the edges of the steel beam became visible. At cycle 16^-, a plastic mechanism formed in the column flanges around the web panel under negative loading. Concrete near the column flange was crushed and a plastic mechanism formed in the column flanges under positive loading of cycle 19^+. The panel zone underwent very large shear distortions, but did not show any sign of distress. At cycles 25 and 26, buckling of the upper and lower flanges of the beam was observed due to large accumulated plastic deformation. A penny-shaped crack was initiated in the lower flange near the cope hole when the load was reversed (cycle 25^+). A decision was made to strengthen the cracked flange by welding two small plates to the flange after cycle 26^-

and the test was continued. The same type of cracking occurred at the upper flange at cycle 27^- and test was finally stopped.

The results of the test are shown by the P-Δ_t diagram in Fig. 8(a), the P-θ_b diagram in Fig. 8(b), and the P-γ_p diagram in Fig. 8(c). A comparison of these diagrams indicates that the panel zone was the weakest element of the specimen and had a dominant influence on the overall behavior, especially after it had been extensively yielded. The specimen exhibited considerable reserve strength beyond web yielding. The participation of the composite beam became increasingly more significant as the controlled displacement increased.

The overall behavior of the specimen may be studied by examining the skeleton curve obtained by connecting the peak points of the hysteresis curves of various levels of displacement. The P-Δ_t diagram of Fig. 8(a) shows that under positive loading there were three distinct ranges of load-deflection behavior: elastic range, transition range and strain-hardening range. The upper limit of the elastic range was at about 120 kN (cycle 12^+ ~ 13^+) and was followed by a substantial reduction in stiffness. The transition range was between cycles 13^+ and 19^+. In this range yielding of the web panel and the composite beam became extensive, followed by formation of a plastic mechanism of the column flanges and crushing of concrete in the contact zone near the column flange. Beyond cycle 19^+ the specimen reached the strain hardening range, after the panel zone as well as the composite beam had strain hardened. The general behavior of the joint under negative loading was similar.

This specimen demonstrated deformation characteristics of a composite joint in that (1) there were remarkable increases in stiffness and strength due to composite action when subjected to positive loading, (2) the

hysteresis loops were very stable but with noticeable pinching due to opening and closing of the concrete cracks, and (3) good ductility existed even after complete crushing of the concrete.

Joint IJ-FC: For this test, in order to simulate the bending and shear conditions existing in a typical interior joint subjected to earthquake loading, the controlled displacements were imposed in opposite directions at the tips of the beams. The amplitudes of the two displacements were always the same and, therefore, the difference in the applied loads P_1 and P_2, reflected the different stiff properties of the composite beam under positive and negative moments.

A total of 37 cycles, the first 15 being nominally elastic cycles, were applied to the specimen in a manner similar to that for EJ-FC. Figure 9(a) shows the hysteresis curves relating the total load, $P_1 + P_2$, applied to the beams and the imposed displacement, Δ_t. The total load is plotted against the panel zone distortion, γ_p, in Fig. 9(b). The sign convention for the loads is shown in Fig. 3.

One third of the web panel showed yielding at cycle 13 and full yielding was observed at cycle 16 at a total load of about 135 kN. At cycle 16, the column flanges surrounding the web panel started to yield and a complete mechanism formed in these flanges with four plastic hinges at the levels of the steel beam flanges. A crack developed in the lower flange near the cope hole of the west beam at cycle 34 and propagated toward to the edges of the flange during the subsequent cycles. Another crack developed in the lower flange of the east beam and the test was terminated at cycle 37. Before testing, the shape of the cope holes in both beams were modified to provide a smoother transition of stresses from the web to the flange. This modification apparently did not prevent the crack development in the

flanges.

The panel zone was again the weakest element in this specimen and the column remained essentially elastic throughout. The overall deflection of the joint was dominated by the shear distortion of the panel zone and the hysteresis loops for Δ_t exhibited the same characteristics as those for γ_p. The hysteresis loops were stable and repetitive and the panel zone showed good ductility with substantial increase in strength beyond initial yielding.

Joint EJ-WC: A total of 22 displacement cycles were applied to the joint and the results obtained are represented as the P-Δ_t curves in Fig. 10(a), the P-θ_b curves in Fig. 10(b), the P-γ_p curves in Fig. 10(c) and the P-Δ_c curves in Fig. 10(d). The results show that the overall behavior of the specimen was affected most significantly by the beam deformation, although the other structural elements also contributed to some extent.

The specimen exhibited linear P-Δ_t behavior up to cycle 15, after which the beam started to yield and the overall stiffness decreased. A local buckle appeared in the lower flange of the beam at cycle 19$^-$ and a drop in the load was immediately observed. The buckling caused unstable hysteretic response in all the subsequent cycles of loading. The joint reached its ultimate load at cycle 19 when the column attained the predicted plastic strength under positive loading and when the beam reached the predicted plastic moment under negative loading. The buckle grew rapidly during the subsequent cycles, although a partial straightening always occurred when the direction of the load was reversed. The over-sized cope hole and the flexibility of the connecting plates, to which the beam flange was attached, were believed to be the important factors causing the buckling. (The beam flanges of EJ-FC and IJ-FC were welded directly to the column flange which

was relatively rigid.) The severely buckled flange was locally strengthened after cycle 21 and the test resumed. Final failure of the joint was due to fracture of the lower flange near the middle of the buckle.

Components of Deflections: The three components of deflection, Δ_b, Δ_c and Δ_p, of the test subassemblages, as determined from the measured data, are shown in Fig. 11. The dominant influence of the panel zone deformation on the overall behavior of EJ-FC and IJ-FC was evident, especially after full yielding of the web panel. In IJ-FC more than 90% of the total deflection was due to panel zone deformation when the applied load exceeded 80% of the maximum load. In EJ-WC the composite beam and the joint panel (column flanges between the connecting plates) contributed almost equal amounts to the total deflection.

DISCUSSION OF RESULTS

Experimental vs. Predicted: Figures 12, 13 and 14 compare the experimental skeleton curves the predicted curves for monotonic loading. The experimental curves were obtained by connecting the peak points of the first cycles of each displacement amplitude. The assumptions made in the predictions are:

(1) Composite Beam

* Effective width of composite slab is one-quarter of beam length.
* Full composite action exists between concrete slab and steel beam.
* Compressive strength of concrete against column flange is 1.3 f_c', where f_c' is the concrete cylinder strength (duPlessis and Daniels, 1972).

* Beam bending theory including shear deformation is valid.
* Shear force is resisted only by the web of steel beam.
* Concrete tensile strength is negligible.
* No strain-hardening occurs.

(2) Panel Zone

* Krawinkler's trilinear model is used (Krawinkler, et al. 1971).
* Panel zone is bounded by D_c x D_b, where D_c is the column depth measured between its flange centerlines and D_b the steel beam depth measured between its flange centerlines when joint is subjected to negative moment and increased as shown in Fig. 15 when subjected to positive moment.
* Distribution of shear stress in the column web depth is uniform.
* von Mises yield criterion is valid.

(3) Column

* Beam bending theory including shear deformation is used.
* No strain-hardening occurs.
* Axial stress is negligibly small.

The no strain-hardening assumption for the beams and columns made above results in perfect plastic hinge formations at their critical locations. For the panel zone, Krawinkler's model assumes that the column flanges in the joint deform elastically after the general yielding of the web panel and their bending stiffness determines the post-elastic stiffness of the joint (the 2^{nd} slope). The column flanges around the web panel is referred to as "Boundary Frame".

Two distinct features may be observed from the comparisons presented. For the case of negative loading (slab in tension), the theoretical

predictions agree quite well with the experimental results. However, for positive loading (slab in compression), the experimental and theoretical results do not agree closely. Details of the comparison for each specimen are summarized below.

Specimen EJ-FC: The overall P-Δ_t relationship under negative loading is in good agreement with the analytical prediction. When positive loading was applied, yielding of the web panel and the boundary frame occurred at loads higher than predicted, but the ultimate strength of the composite beam at the connection was less than predicted, using the available theory (duPlessis and Daniels, 1972). These discrepancies may be explained as follows:

* The bolted web connection was designed for the total shear force under combined gravity and earthquake loading. The design satisfied the requirements of the American Institute of Steel Construction (AISC) Specification (Specification for design, fabrication and erection of structural steel for buildings, 1978), but the shear capacity of the connection was only 50% of the capacity of the beam web. This capacity was sufficient to resist the shear accompanying the negative loading, but was probably insufficient to resist the positive loading shear.

* Effects of composite slab on the yield strength and on the post-yield stiffness of the composite joint panel zone were higher than the predicted.

Specimen IJ-FC: As shown in Fig. 9, the overall behavior of this specimen was dominated by the shear deformation of the panel zone. The experimental strength was higher than the predicted in the post-yield range of the panel zone. This difference in strength was caused mainly by the effect of composite slab on the panel zone yield strength, but strain hardening

probably was also a contributing factor.

Specimen EJ-WC: The predicted stiffness and strength show good agreement with the experimental results for both positive and negative loading. Despite early buckling of the beam flange, the specimen achieved the predicted maximum load under negative loading and exceeded by about 10% the predicted value under positive loading.

Behavior of Composite Beams

Stiffness: Figure 16 shows the comparison between the experimental and predicted $P\text{-}\theta_b$ relationships of the composite beam of specimen EJ-FC. The experimental elastic stiffness under negative moment is higher than the predicted, based on I^-_{com} for the steel beam plus reinforcing steel within an effective width equal to one quarter of the beam span. The difference is 13.6%. Under positive moment, the experimental stiffness is 106% of the theoretical stiffness of the bare steel beams, but only 74% of the value calculated for the fully composite section with an effective slab width of one-quarter of the beam length.

Strength: Under negative loading, the experimental moment capacity of the composite beam of EJ-FC is 10.6% higher than the capacity of the bare steel beam, even though theoretical calculations show that the weak bolted web connection would reduce the moment capacity of the beam by 18%. The predicted positive moment capacity, shown in Fig. 16, is based on a concrete compressive strength of 1.3 f'_c and is 21% higher than the experimental capacity. This difference, however, becomes less than 2% if the shear strength of the bolted web connection is taken into account.

Hysteretic Behavior: The experimentally determined moment-curvature relationships of a section 260 mm from the column face of EJ-FC is presented

in Fig. 17. There was little change in stiffness when the stresses remained in the elastic range. In the inelastic range the overall behavior showed the characteristics of both the concrete slab and steel beam. The deterioration of stiffness under positive moment and the stable hysteresis loops under negative moment were evident. The skeleton curve of the moment-curvature relationship would be bilinear. The strain-hardening slope under negative moment would be about 3.0% of the elastic stiffness and that under positive moment about 1.0%. After inelastic deformation under positive moment, the unloading tangent stiffness was initially the same as the elastic positive stiffness, but gradually reduced to the stiffness of the bare steel beam. The reloading curve in the negative moment region showed markedly the Bauschinger effect and eventually traced the negative skeleton curve. When the direction of load was reversed after negative inelastic deformation, the bending moment was carried by the bare steel beam in combination with the reinforcing bars. If the negative inelastic deformation that had been reached before load reversal was very large, the steel beam would yield under positive moment prior to the closing of the concrete cracks. In this case, the hysteresis curve would have the characteristics same as those in the negative moment region. After the slab cracks were closed sufficiently, the beam would gain stiffness and the moment-curvature curve would eventually trace the positive skeleton curve.

Behavior of Panel Zone

Elastic Stiffness: Figure 15 shows a positive moment M_b^+ and a negative moment M_b^- acting on an interior joint panel zone. Each of these moments may be replaced by two equal and opposite forces $Q = M_b/D_b$. For a bare steel beam, D_b becomes the distance between the centerlines of the

upper and lower flanges or d_b. The shear force, V_p, of the panel zone, is

$$V_p = \frac{M^+_b}{D^+_b} + \frac{M^-_b}{D^-_b} - V_c \qquad (2)$$

in which V_c is the column shear. The elastic stiffness K_e of the panel zone is the ratio of V_p to the average shear distortion, γ_p

$$K_e = \frac{V_p}{\gamma_p} \qquad (3)$$

In a composite joint, the presence of the slab increases the stiffness of the panel zone, because of the enlarged panel zone size. A comparison of the stiffnesses of the panel zone of EJ-FC under positive and negative bending moments shows clearly this behavior (Fig. 18). From the experimental stiffness of the panel zone of EJ-FC under positive moment, it is possible to find the D_b^+ distance for the composite beam. The value of D_b^+ thus determined is 28.9% larger than the depth of the bare steel beam d_b. The D_b^+ depth is close to the distance measured from the centerline of the concrete slab to centerline of the lower flange.

Shear yielding of web: Using the von Mises yield criterion and the D_b^+ and d_b values defined above, the shear yield strengths of the panel zone webs of EJ-FC and IJ-FC have been calculated and compared with the experimental results. For EJ-FC, the calculated value is higher by 8% for positive loading and 12.5% for negative loading. For IJ-FC the calculated value is higher by 7%. Both the experimental and calculated results indicate that the shear yield strength under positive loading is increased approximately by the ratio of D_b^+ to d_b.

Post-yield behavior: It has been know that panel zones have high

reserve strength beyond web yielding (Krawinkler, et al. 1971). The post-yield behavior of the panel zone of the test specimens observed during the tests may be summarized as follows: (1) A plastic hinge mechanism formed gradually in the boundary frame at relatively large deformations (γ_p = 0.015 to 0.020 radians.) (2) The formation of the plastic mechanism reduced significantly the panel zone stiffness, (3) Plastic hinges formed at the same locations for both positive and negative loading, and (4) Under positive bending, composite slab caused an increase in the shear strength of the panel zone even at large distortions. The increase was almost constant (38 to 43%) between the yield distortion γ_y and a distortion of 0.02 radians.

Ductility: The composite panel zones in the test specimens showed very ductile behavior, much like the panel zones in steel joints, (Naka, et al. 1967, Krawinkler, et al. 1971, Lu, et al. 1985). Ductility ratios, γ/γ_y, of more than 30 were observed in the tests before the composite beam failed by fracture.

Energy Dissipation Capacity: One of the important considerations in evaluation of the performance of a structure subjected to severe earthquake motions is its energy dissipation capacity. This capacity is generally displacement dependent and serves as an indication of the structure's ability to dissipate energy through inelastic deformation. The dissipated energy per displacement cycle U_D is determined as the area under the load-displacement diagram. Figure 19 shows the dissipated energy of specimens EJ-FC and EJ-WC calculated from the test results. The energy per cycle is separated into two parts, U_D^+ for positive loading and U_D^- for negative loading. It is evident that the increase in energy dissipation capacity due to composite action is small and that EJ-WC, because of early flange

buckling and fracture, dissipated less energy than EJ-FC. The latter has also been observed in the earlier tests on steel beam-to-column connections (Popov and Pinkney, 1969).

CONCLUSIONS

The following conclusions may be drawn from the results presented; they are applicable to composite joint subassemblages with dimensions, member sizes and fabrication details similar to those of the test specimens.

(1) Under positive bending, the composite action of floor slab may increase substantially the stiffness and strength of steel beams in a joint subassemblage. The increase in stiffness may diminish somewhat under repeated load reversals.

(2) The stiffness and strength of a panel zone under positive loading are also increased substantially by the composite action of slab. The results of EJ-FC test showed a 29% increase in both the elastic stiffness and yield strength of the web panel, which is about the same as the increase of beam depth from d_b to D_b^+.

(3) The web panel and its boundary frame in a composite joint can deform inelastically through large shear distortions. Panel zone rotations of 0.05 ~ 0.07 radians (5 ~ 7% distortion) were achieved in EJ-FC and IJ-FC before fracture occurred in the beam flanges near the cope holes.

(4) The hysteresis curves of EJ-FC and IJ-FC were stable and repetitive, but showed a slight pinching at large displacements. The opening and closing of the cracks in the concrete slab under load reversals are the primary causes of the pinching.

(5) The maximum total deflections Δ_t reached in the three specimens represented a story drift index in the range of 0.024 to 0.044. This is

much larger than the story drifts reached during the testing of the prototype structure and may explain why no fracture was ever observed in any of the connections.

(6) The over-sized cope holes are believed to be the cause of the beam flange fracture in all the specimens. Previous tests on steel beam-to-column joints having similar member sizes but with smaller cope holes did not show the type of fracture observed.

(7) The over-sized holes in the beam web and the connecting plates in EJ-WC apparently allowed the compression flange of the composite beam to buckle early. This buckling resulted in unstable hysteretic behavior and led to eventual fracture of the beam flanges.

(8) The bolted web connections in EJ-FC and IJ-FC were found to be insufficient to resist the shear force present in the joint when it was subjected to the maximum positive bending moment. This indicates that if the increase in the positive moment capacity due to composite action is to be utilized in design, care is necessary to insure that the web connection has adequate strength to resist the accompanying shear.

(9) Because of the pinched character of the hysteresis curves of joints subjected to positive loading, it has been shown that there is only a small increase in energy dissipation capacity due to composite action.

(10) In moment-resisting frames designed according to the weak-beam and strong-column concept, it may be beneficial to allow limited yielding to occur in the panel zone in order to lessen the ductility demand on the beams and the connecting elements.

As a result of this investigation, hysteretic models for composite beams and composite joint panel zones have been developed and implemented in the available dynamic analysis computer programs, the details of which are

presented elsewhere (Lee, 1987, Lu, et al. 1988).

ACKNOWLEDGMENTS

This research described in this paper was supported by the National Science Foundation through Grant Nos. PFR-8008587 and CEE-8207712 and was part of the "U.S. - Japan Cooperative Earthquake Research Program Utilizing Large-Size Testing Facilities," initiated by Joseph Penzien and Hajime Umemura. During the course of investigation, the program was coordinated by Robert D. Hanson and Makoto Watabe. The valuable support and advice provided by Drs. Michael P. Gaus, S. C. Liu and John B. Scalzi of the NSF are gratefully acknowledged. The findings and opinions expressed are those of the authors and do not necessarily represent the views of the sponsor.

APPENDIX 1 - REFERENCES

Askar, G., Lee, S. J., and Lu, L. W. (1983). "Design studies of the six-story steel test building". Report No. 467.3, Fritz Engrg. Lab., Lehigh Univ., Bethlehem, PA.

duPlessis, D. P. and Daniels, J. H. (1972). "Strength of composite beam-to-column connections". Report No. 374.3, Fritz Engrg. Lab., Lehigh Univ., Bethlehem, PA.

Foutch, D. A., Goel, S. C., and Roeder, C. W. (1987), "Seismic testing of a full-scale steel building - part I". J. Struct. Engrg., ASCE, 113(11), 2111 - 2129.

Krawinkler, H., Bertero, V. V., and Popov, E. P. (1971). "Inelastic behavior of steel beam-to-column subassemblages". Report No. UCB/EERC 71-7, Earthquake Engineering Research Center, Univ. of California, Berkeley.

Lee, S. J. (1987). "Seismic behavior of steel building structures with composite slabs". Thesis presented to Lehigh Univ. at Bethlehem, PA in partial fulfillment of the requirements for the degree of Doctor of Philosophy.

Lu, L. W., Slutter, R. G. and Lee, S. J. (1985). "Ductility and fracture of joints with panel zone deformation". Symposium report, IABSE-ECCS symposium on "Steel in Buildings", Luxembourg.

Lu, L. W., Wang, S. J., and Lee, S. J. (1988). "Cyclic behavior of steel and composite joints with panel zone deformation". Paper presented at the Ninth World Conference on Earthquake Engineering, Tokyo, Japan, (to appear in the conference proceedings).

Naka, T., Kato, B. and Watabe, M. (1967). "Research on behavior of steel beam-to-column connections". Technical report, Laboratory for Steel Structures, Department of Architecture, University of Tokyo, Japan.

Plumier, I. A. (1983). "Recommended testing procedure for evaluating earthquake resistance of structural elements". European Convention for Constructional Steelwork, Technical Committee 13, Brussels, Belgium.

Popov, E. P. and Pinkney, R. B. (1969). "Cyclic yield reversals in steel building joints". J. Struct. Div., ASCE, 95(3), 327 - 353.

Roeder, C. W., Foutch, D. A., and Goel, S. C. (1987). "Seismic testing of a full-scale steel building - part II". J. Struct. Engrg., ASCE, 113(11), 2130 - 2145.

Specification for the design, fabrication and erection of structural steel for buildings (1978). American Institute of Steel Construction, Chicago, IL.

Standards for design of steel structures (1970). Architectural Institute of Japan, Tokyo, Japan.

APPENDIX 2 - NOTATION

D_b = beam depth

D_c = column depth

d_c = depth of bare steel beam

f'_c = compressive strength of concrete

I = moment of inertia of beam

K_e = elastic stiffness of panel zone

K_o = elastic on initial slope

L = beam length

M_b = beam bending moment

P = load applied at tip of beam

P_y = yield load

U_D = dissipated energy per cycle

V_c = column shear

V_p = panel zone shear

γ_p = panel zone distortion

Δ_b = drift due to beam deformation

Δ_c = drift due to column deformation

Δ_p = drift due to panel zone deformation

Δ_y = yield deflection

Δ_t = total deflection on drift

θ_b = rotation of beam

σ_y = yield stress of steel

τ_y = shear yield stress

ϕ = curvature

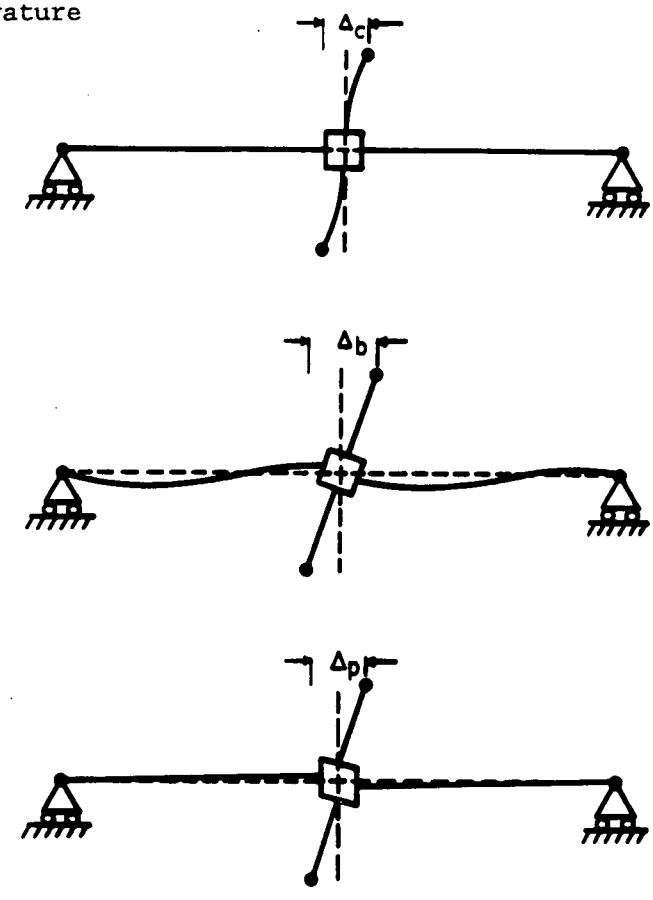

Fig. 1. Components of Story Drift

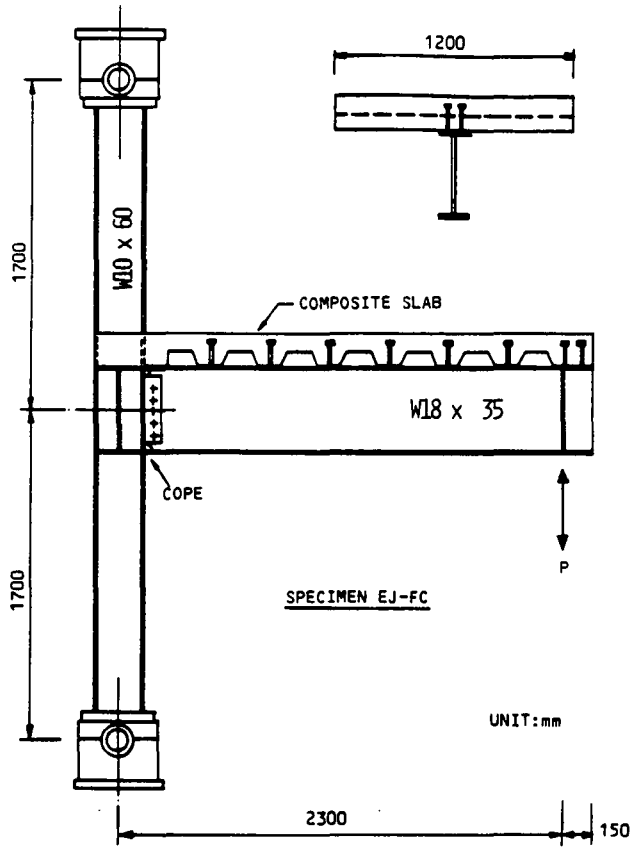

Fig. 2. Dimensions and Members Sizes of EJ-FC

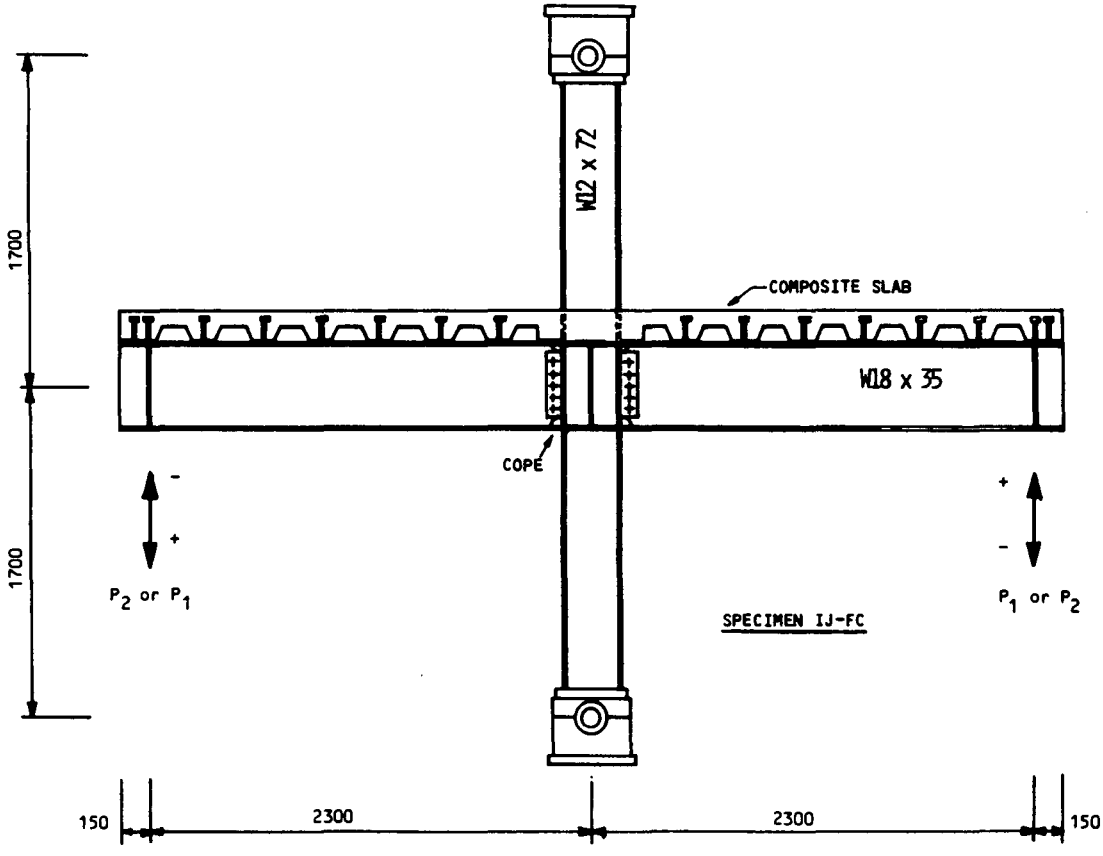

Fig. 3. Dimensions and Member Sizes of IJ-FC

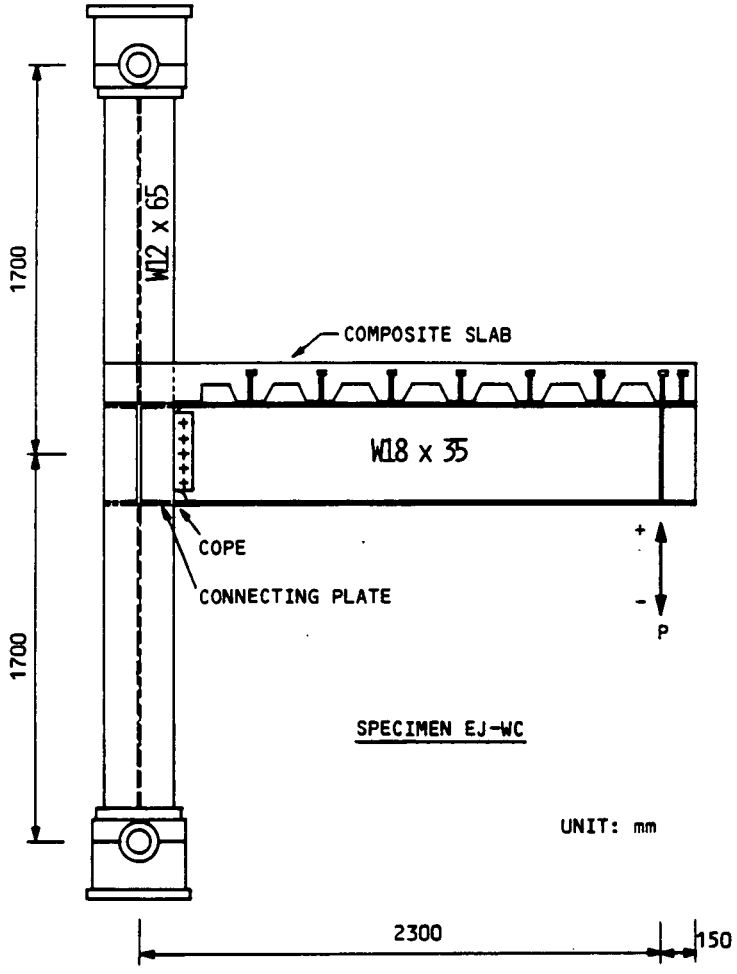

Fig. 4. Dimensions and Members Sizes of EJ-WC

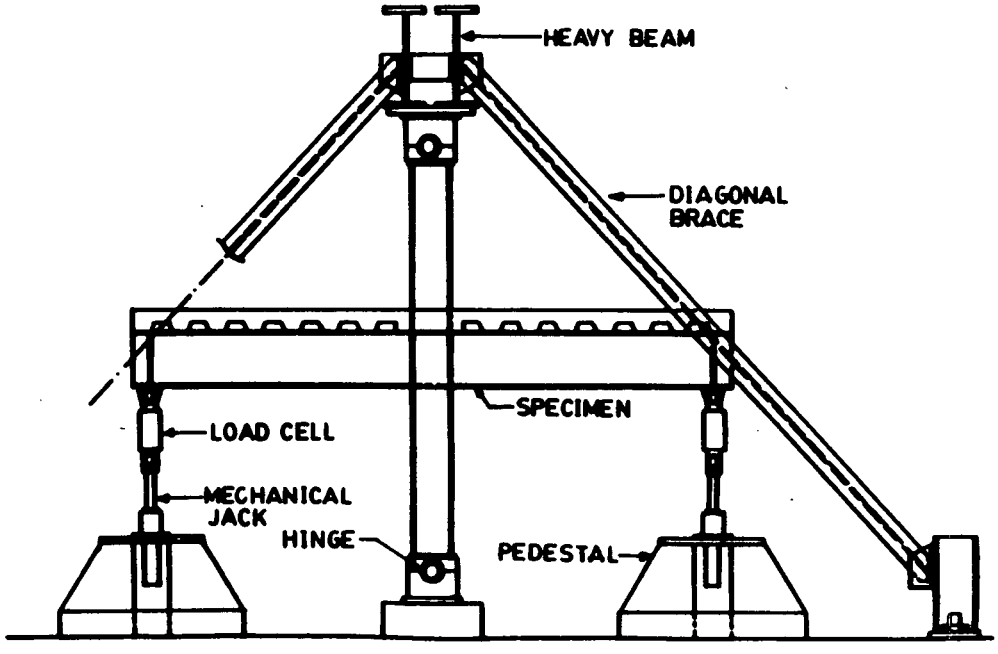

Fig. 5. Test Setup

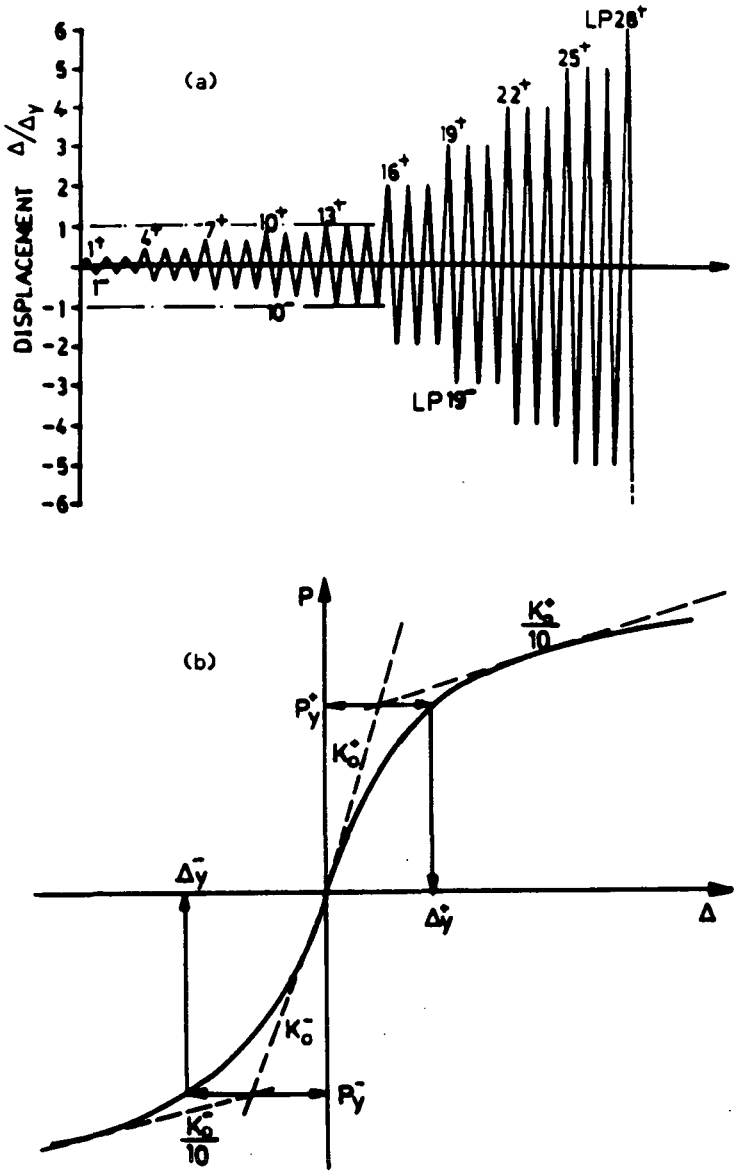

Fig. 6. Selection of Controlling Displacements

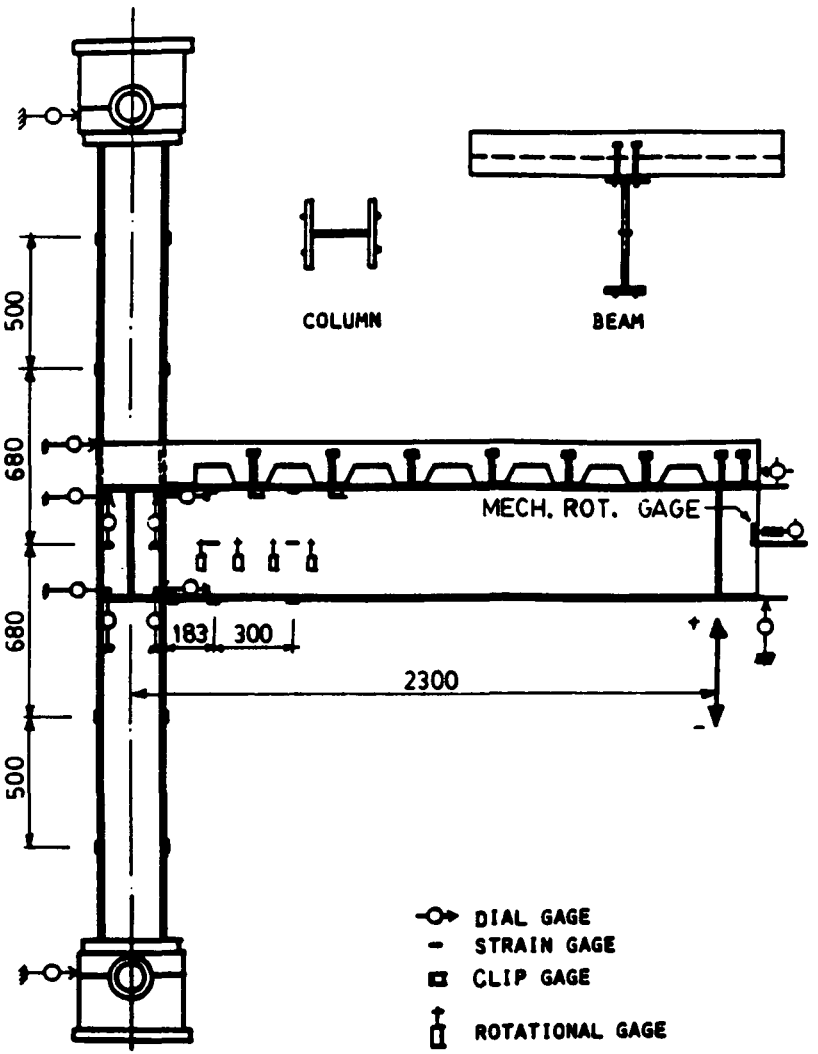

Fig. 7. Instrumentation of EJ-FC

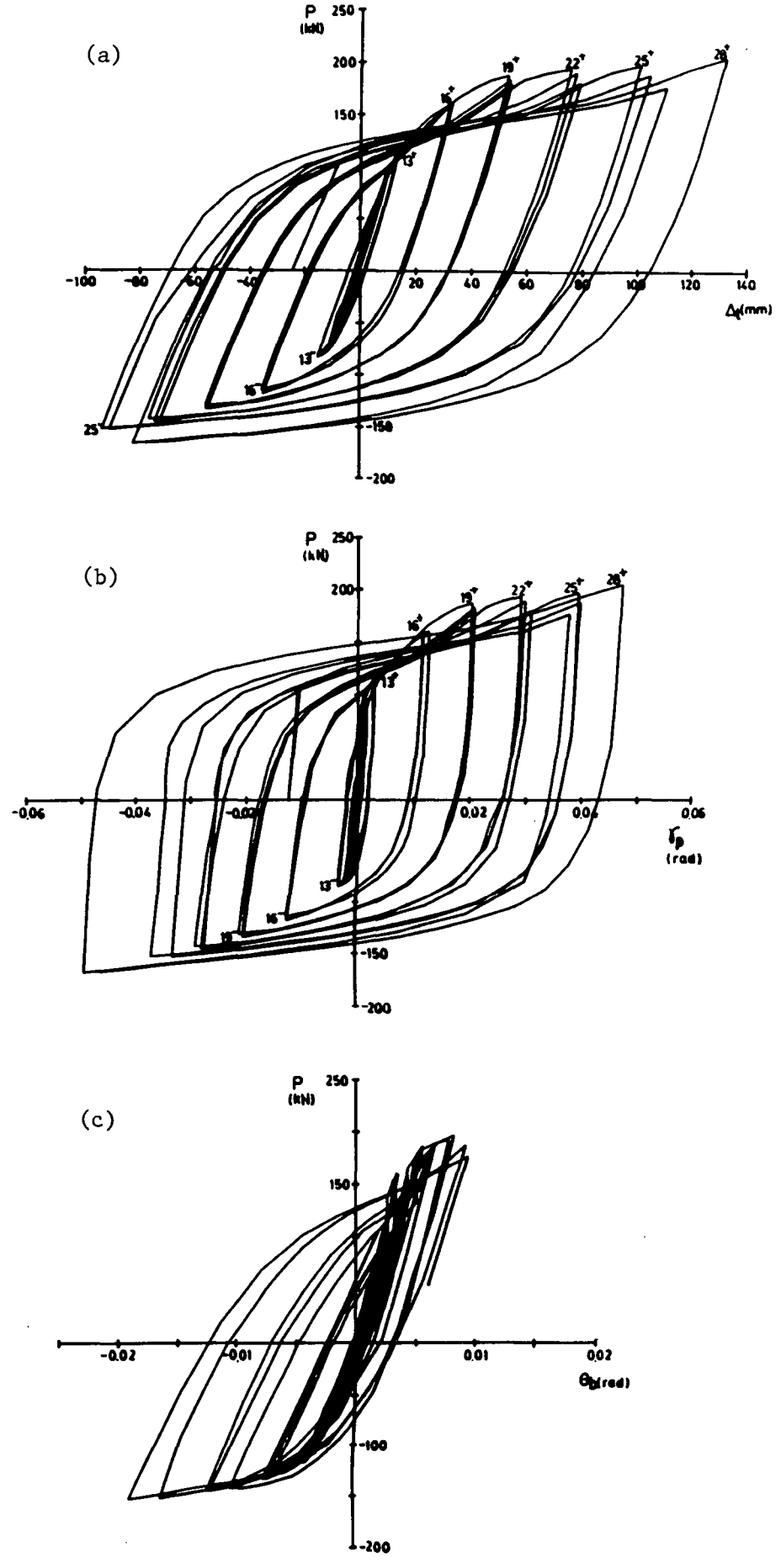

Fig. 8. Results of EJ-FC Test

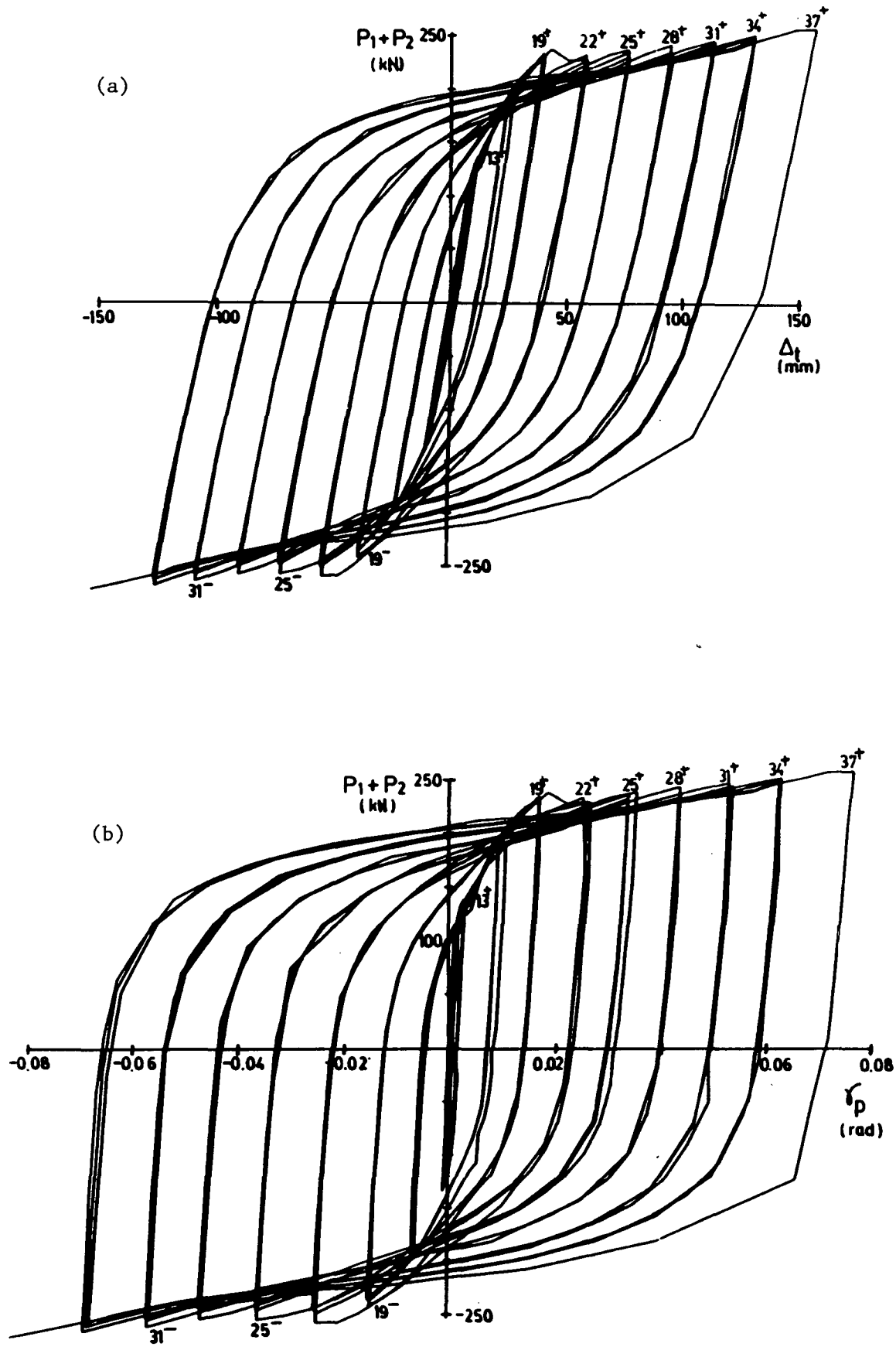

Fig. 9. Results of IJ-FC Test

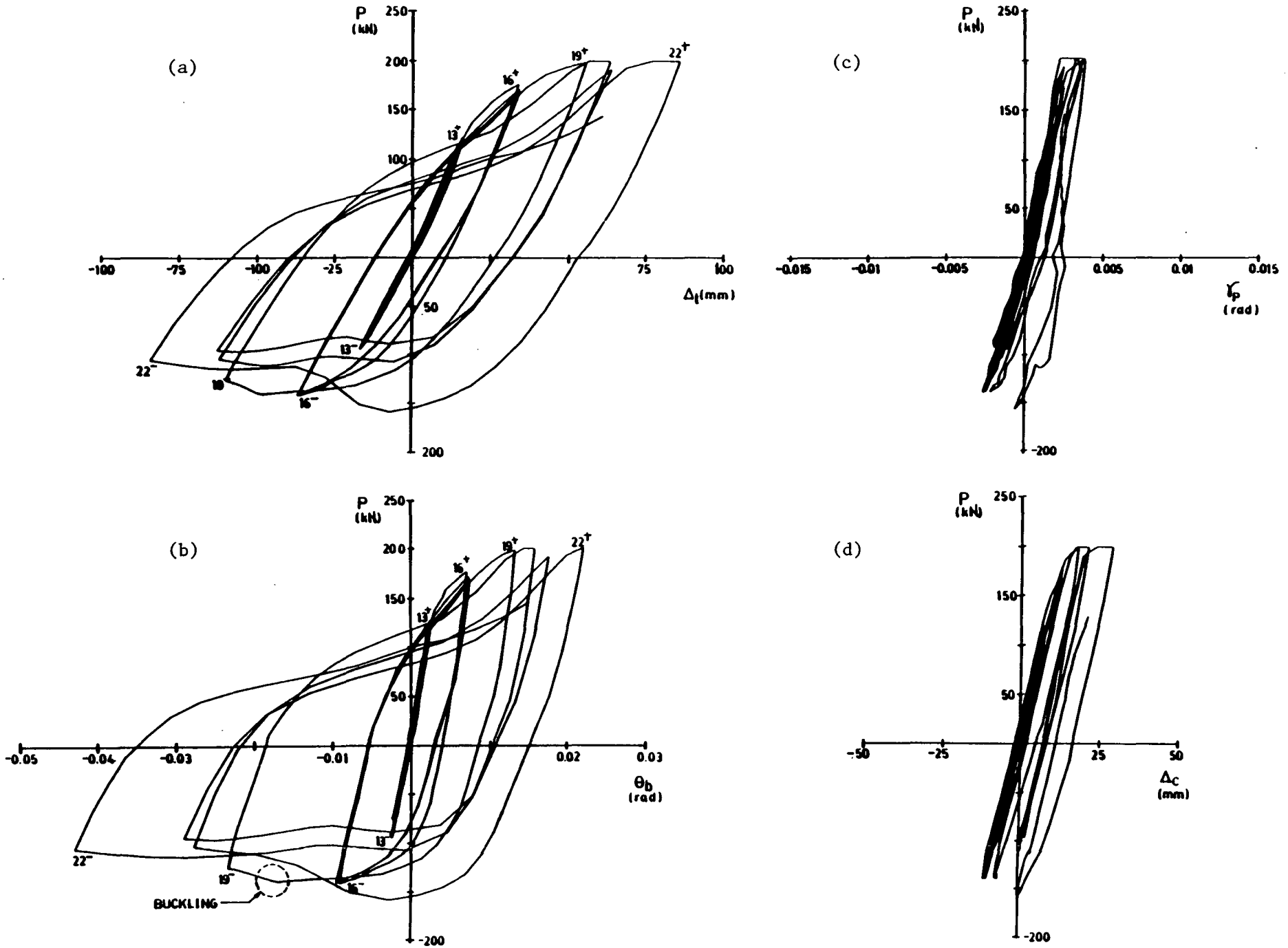

Fig. 10. Results of EJ-WC Test

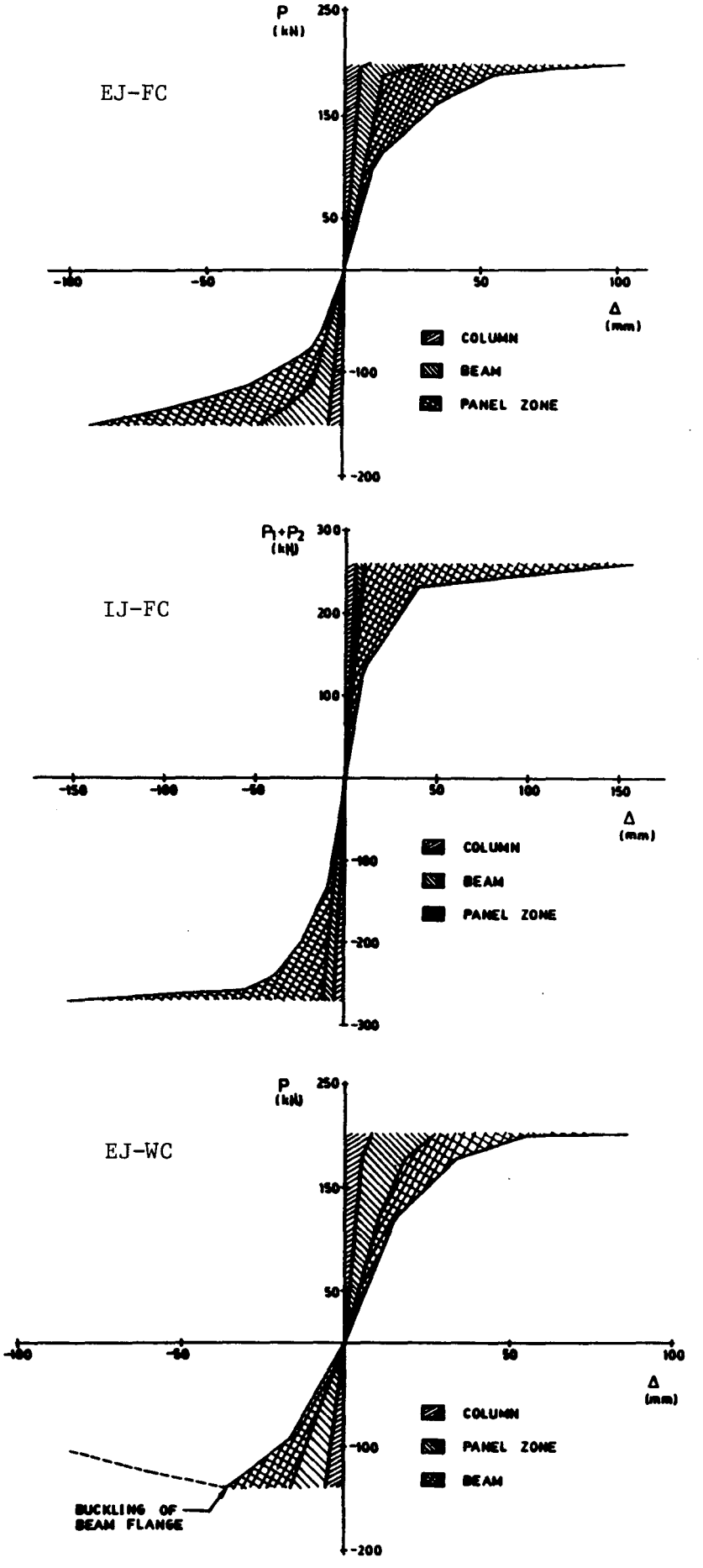

Fig. 11. Deflection Components of Test Specimens

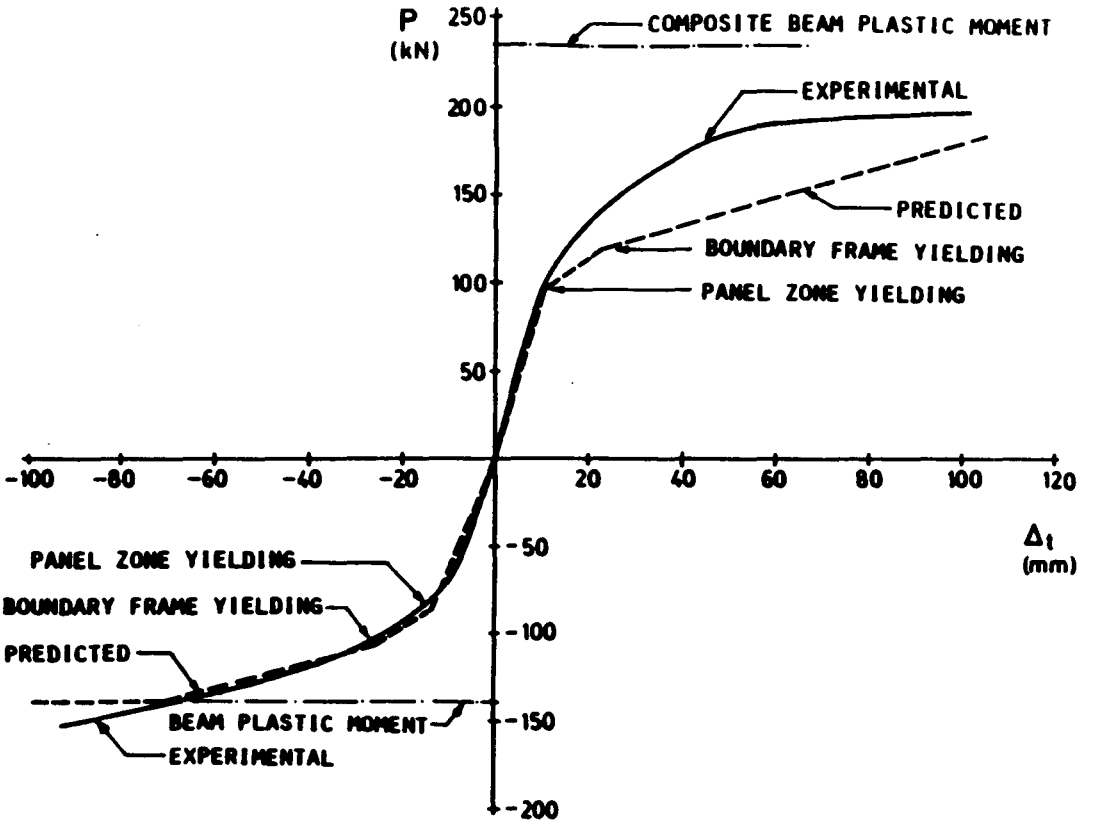

Fig. 12. Experimental vs. Predicted P-Δ_t Curves of EJ-FC

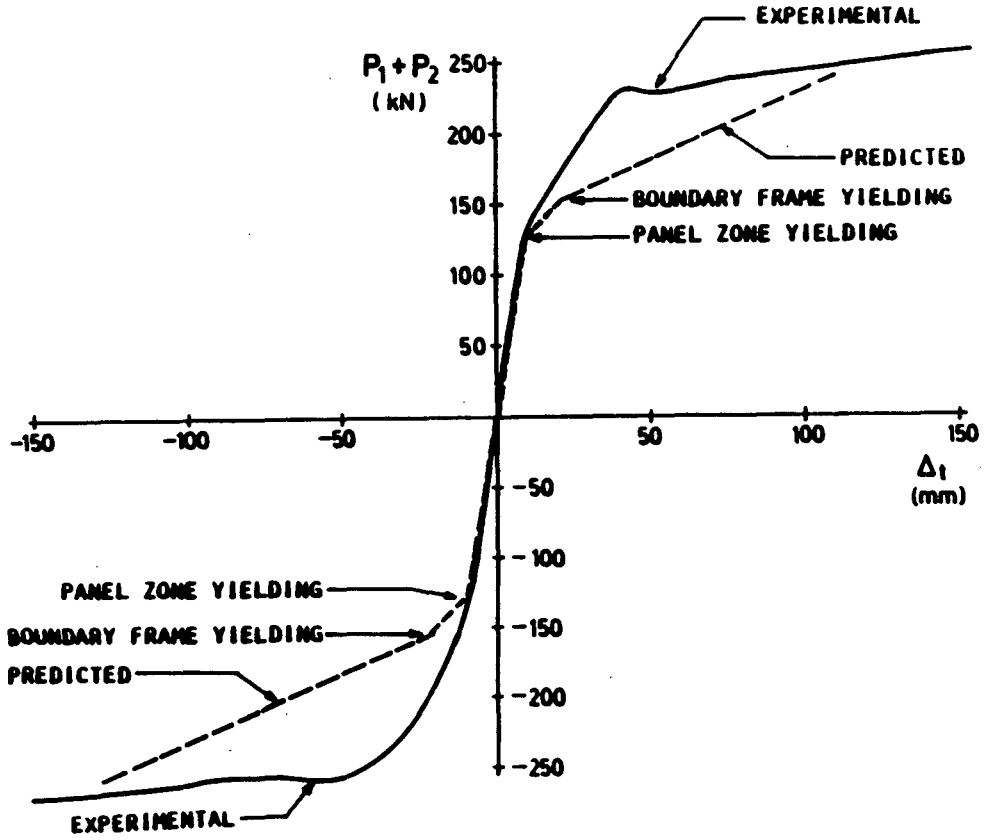

Fig. 13. Experimental vs. Predicted P-Δ_t Curves of IJ-FC

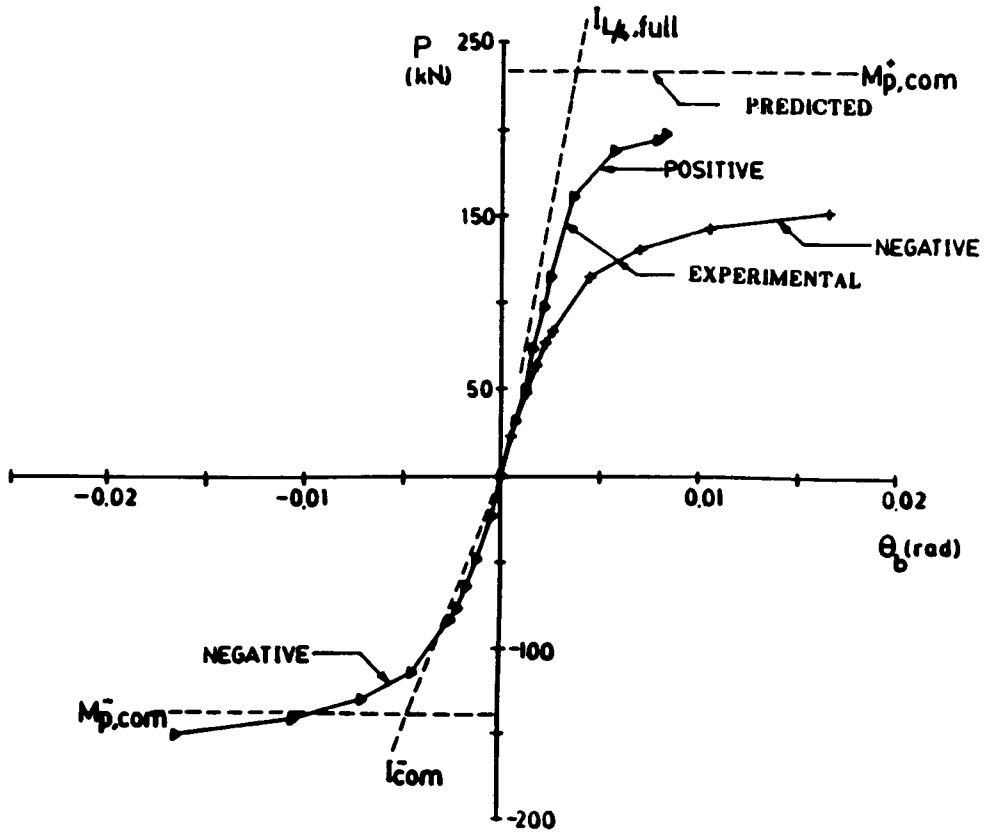

Fig. 16. Skeleton Curves of Composite Beam Rotation of EJ-WC

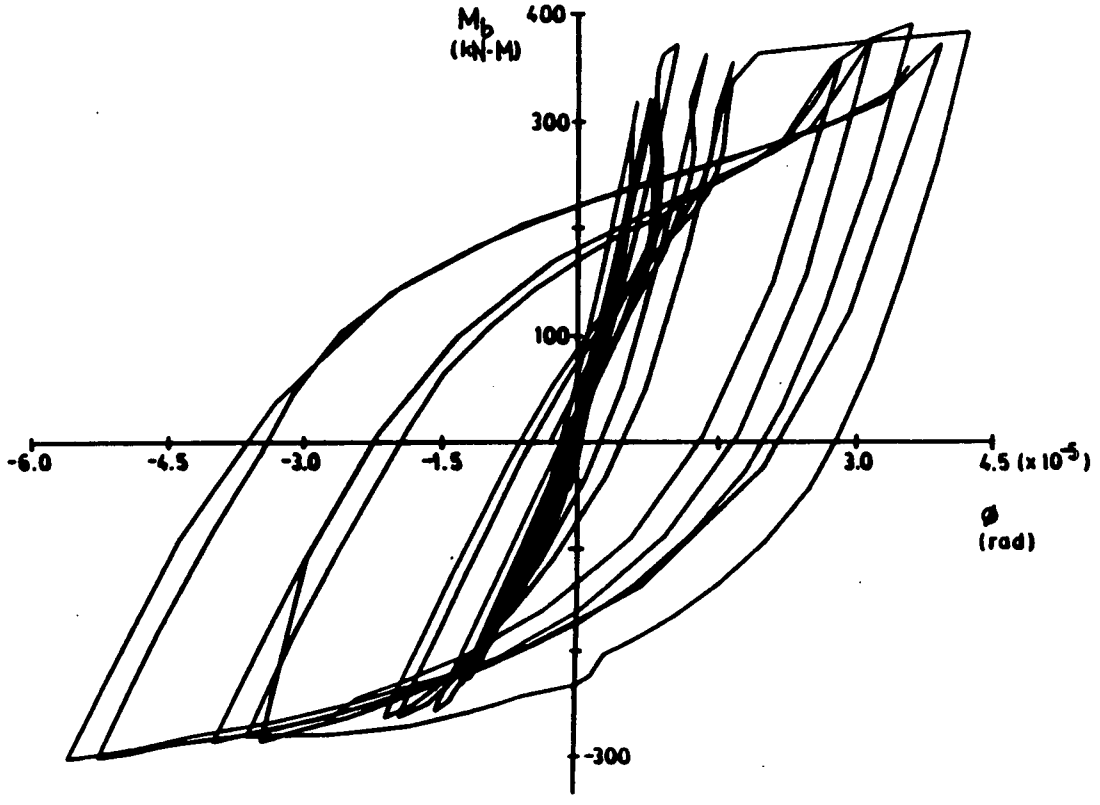

Fig. 17. Moment-Curvature Curves of Composite Beam of EJ-FC

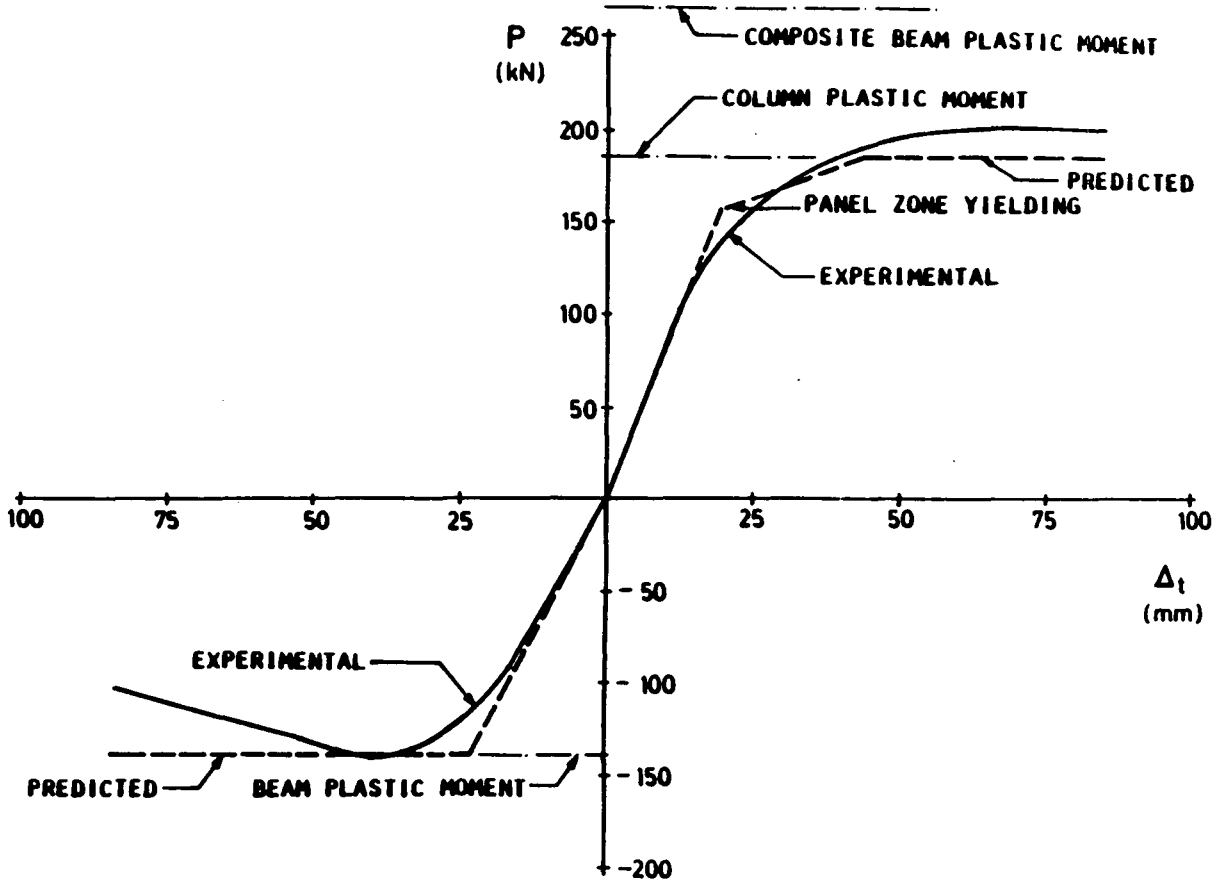

Fig. 14. Experimental vs. Predicted P-Δ_t Curves of EJ-WC

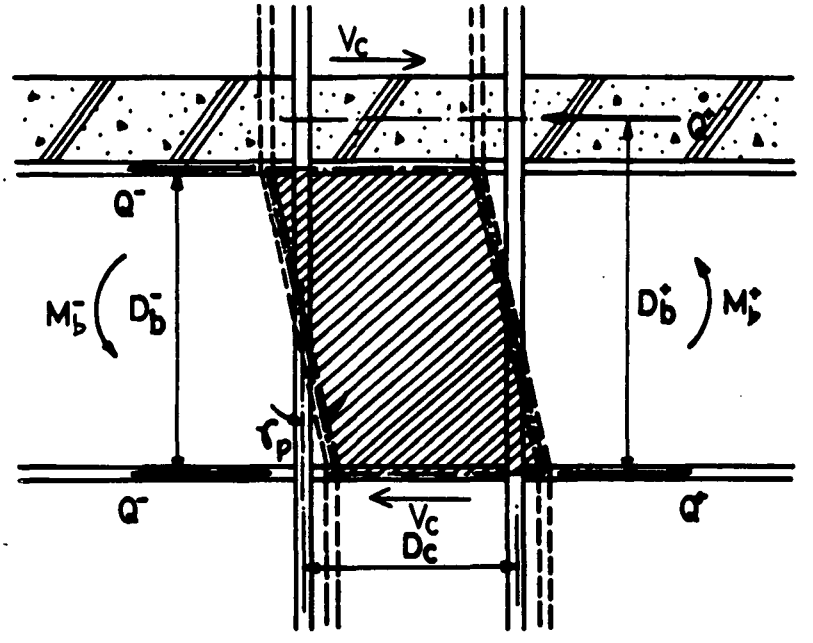

Fig. 15. Joint Panel Zone Deformation

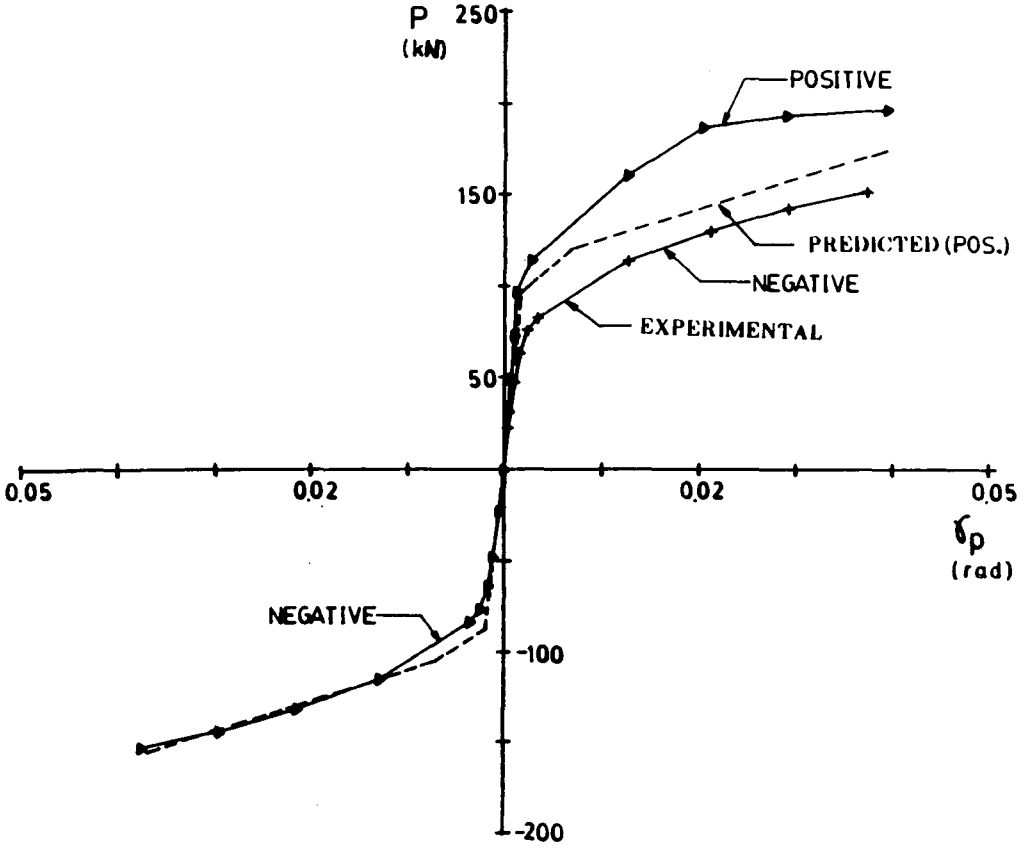

Fig. 18. Skeleton Curves of Panel Zone Deformation of EJ-FC

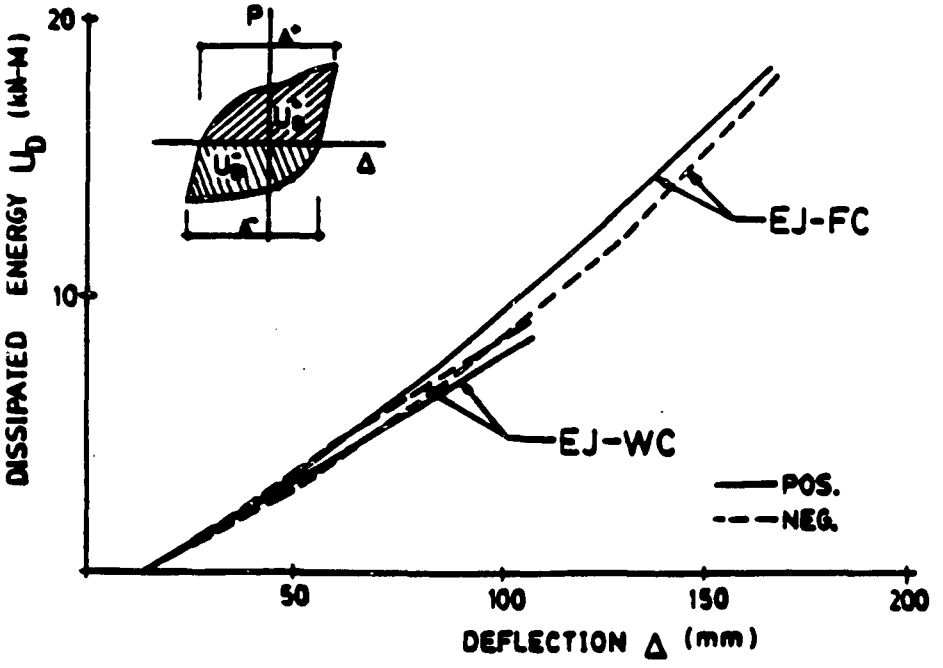

Fig. 19. Energy Dissipation of EJ-FC and EJ-WC

KEY WORDS

Steel structure, earthquake, joint, panel zone, beam, column, stiffness, strength, ductility, energy dissipation capacity.

SUMMARY

Selected results of cyclic tests of three full-scale composite beam-to-column joint subassemblages are presented. The purpose of the tests is to study the stiffness, strength, ductility and energy dissipation of the subassemblages with emphasis on the effects of composite slab and panel zone deformation.